BIOCHEMISTRY
including biophysical chemistry & molecular biology
Current Topic

Biochemistry **2010,** *49,* 7417–7427 7417
DOI: 10.1021/bi100901h

Mechanistic Diversity of Red Fluorescence Acquisition by GFP-like Proteins[†]

Rebekka M. Wachter,* Jennifer L. Watkins, and Hanseong Kim

Department of Chemistry and Biochemistry, Arizona State University, Tempe, Arizona 85287-1604

Received June 3, 2010; Revised Manuscript Received July 22, 2010

ABSTRACT: This review aims to summarize our current state of knowledge of several post-translational modification mechanisms known to yield red fluorescence in the family of GFP-like (green fluorescent protein-like) proteins. We begin with a brief review of the maturation mechanism that leads to green fluorescence in GFPs. The main body of this article is focused on a series of main chain redox and β-elimination reactions mediated by light and O_2, ultimately yielding a red-emitting chromophore. In all GFP-like proteins, a tyrosine-derived phenolic group constitutes an essential building block of the chromophore's skeleton. Two major classes of red-emitting species have been identified in naturally occurring fluorescent proteins. In the DsRed type, an acylimine moiety is found to be conjugated to the GFP-like chromophore. Recent evidence has suggested that two mechanistic pathways, a green branch and a red branch, diverge from an early cyclic intermediate that bears a standard tyrosine side chain. Therefore, the long-standing notion that all FP colors originate from modifications of the GFP-like chromophore may need to be revised. In the Kaede-type green-to-red photoconvertible class of FPs, a light-mediated main chain elimination reaction partakes in the formation of a three-ring chromophore that involves the incorporation of a histidine residue into the conjugated system. A mechanistic role for photoexcitation of the GFP-like chromophore is undisputed; however, the nature of associated proton transfer steps and the charge state of the critical imidazole group remain controversial. In addition to the two major classes of red fluorescent proteins, we briefly describe yellow fluorescence arising from modifications of DsRed-type intermediates, and the less well understood photoactivated oxidative redding phenomenon.

Fluorescence generated by green fluorescent protein-like proteins has naturally evolved to encompass the full visible spectrum. The ability of fluorescent proteins (FPs)[1] to emit visible light stems from a post-translational self-modification of three consecutive amino acid residues that adopt a distorted helical conformation in the interior of the native protein (*1*). When this tripeptide is subjected to a series of autocatalytic steps involving O_2-dependent and O_2-independent processes, a light-responsive chromophore is generated. The extent of bond desaturation within the chromophore coupled with the chemical environment of the surrounding protein matrix dictates the wavelength of light emitted by the protein. Manipulation of these parameters has allowed for color tuning within the visible and near-visible range of electromagnetic radiation, and a broad variety of engineered FPs are currently available as research tools in biotechnology (*2*, *3*).

The GFP folding topology consists of a barrel-shaped domain, in which 11 β-strands assemble to enclose a helical structure that may or may not bear a chromophore (Figure 1A). Aside from GFP-like proteins, this fold has been identified in human extracellular matrix proteins. In these proteins, the 11-strand β-barrel termed G2F (globular-2) fragment is part of a multidomain protein and provides a binding surface for protein−protein interactions (*4*). Therefore, two major gene lineages harbor proteins adopting the GFP fold within the kingdom animalia, the colorless G2F lineage and the GFP-like lineage (Figure 1B). These two branches of the protein superfamily tree are thought to have originated from a common ancestor that predates the divergence of Radiata (phylum Cnidaria) and Bilatera (phyla Arthropoda, Chordata, etc.) (*5*).

Within phylum Cnidaria, class Hydrozoa entails jellyfish bearing GFP and GFP-like proteins, whereas class Anthozoa entails four ancient FP clades that exhibit extensive color diversification (Figure 1B) (*6*, *7*). Clade A has been assigned to order Actiniaria comprising the sea anemones, and clades B−D have been assigned to order Scleractinia comprising the reef-building or stony corals. Most known extant red fluorescent proteins belong to clades C and D, whereas clade B constitutes a lineage with functional specialization related to the purple phenotype, essentially nonfluorescent chromoproteins (*7*). Red fluorescent proteins within clades C and D are thought to have undergone evolutionary lineage sorting into either DsRed-type along clade C or Kaede-type along clade D (*7*) (Figure 1B). Regardless, the common ancestor to all coral fluorescent proteins is thought to be of the green phenotype (*8*), whereas color diversification appears to be a more recent event that occurred upon positive selection for specific color classes in response to environmental pressures (*9*). Although over the years a variety of evolutionary driving forces have been suggested, the biological purpose and necessity for specific color classes remain poorly understood (*9*).

This review is centered on delineating our current understanding of the mechanism of red fluorescence acquisition by

[†]This work was supported by a grant from the National Science Foundation (NSF MCB-0615938) to R.M.W.

*To whom correspondence should be addressed. E-mail: rwachter@asu.edu. Phone: (480) 965-8188. Fax: (480) 965-2747.

[1]Abbreviations: FP, fluorescent protein; GFP, green fluorescent protein; G/R, green-to-red; ESPT, excited-state proton transfer; PDB, Protein Data Bank.

Published on Web 07/28/2010

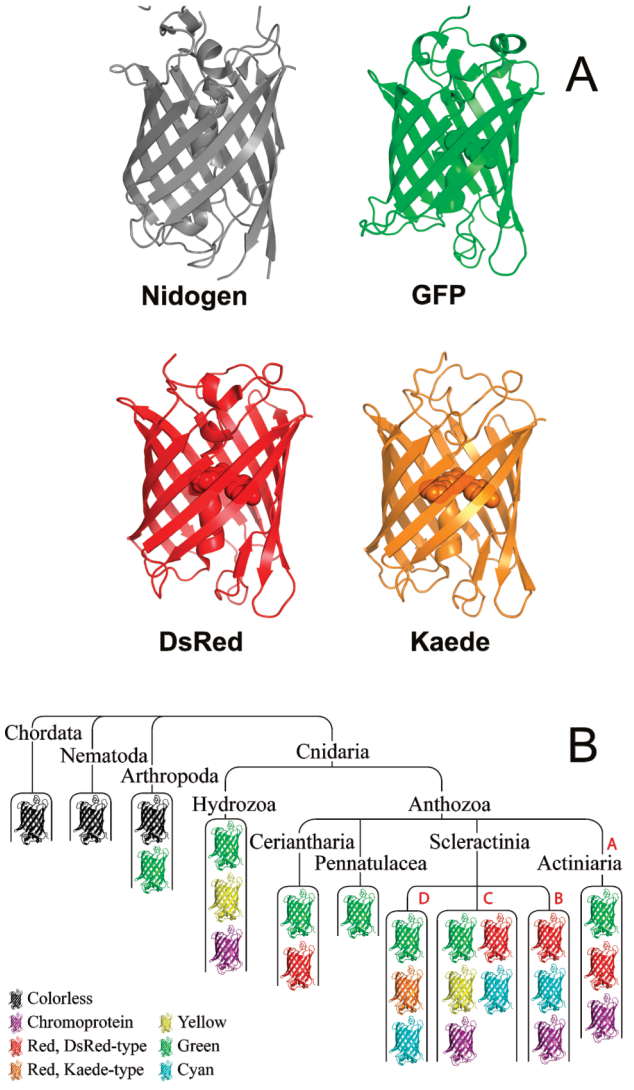

FIGURE 1: (A) Protein folding topologies are shown for several color representatives, using Protein Data Bank entries 1H4U (nidogen, gray), 1GFL (GFP, green), 1ZGO (DsRed, red), and 2GW3 (Kaede, G/R photoconvertible). The respective π-conjugated systems of the chromophore are shown as space-filling models. (B) Outline of major phylogenetic branches of the superfamily protein tree in relation to color evolution in GFP-like proteins, after Alieva et al. (*7*). Clades A−D of class Anthozoa are indicated by capital red letters. Proteins that adopt the GFP fold but are devoid of a chromophore are colored gray.

naturally occurring GFP-like proteins and their variants, with a primary focus on DsRed-type and Kaede-type red fluorescence. Although many of the mechanistic details remain unanswered in this rapidly evolving field, substantial advances have been made in our understanding of the variety of biosynthetic processes mediated by the GFP β-barrel fold. We will begin with a brief review of the protein self-processing mechanism that confers green fluorescence upon some FPs and then expand on several mechanistic themes related to the biogenesis of red-emitting chromophores, emphasizing main chain redox reactions and light-mediated β-elimination reactions. We have included a short discussion of yellow and orange FPs, as well as a brief summary of photochemical and redox phenomena related to the conversion of green-fluorescing proteins to red-emitting forms.

Over the past decade, extensive protein engineering efforts have provided an impressive array of red and far-red fluorescent proteins useful in deep tissue imaging of mammals (*10*), useful in the live cell observation of single-molecule dynamics (*11*), and useful in the provision of photoactivatable tools for super-resolution microscopy (*12*). For an extensive compilation of currently available red fluorescent proteins, listed in combination with their biochemical and optical properties, the reader is referred to several recent review articles and commentaries (*2*, *3*, *12*, *13*), as well as a recent article focused entirely on far-red FPs (*10*).

BIOGENESIS OF THE GFP-LIKE CHROMOPHORE PROCEEDS VIA A CYCLIC IMINE INTERMEDIATE

In green fluorescent proteins, the transition from the natively folded precursor protein to the green fluorescing mature form is governed by three major chemical steps. In avGFP, which is derived from the Pacific Northwest jellyfish *Aequoria victoria*, the functional tripeptide consists of a Ser-Tyr-Gly sequence in positions 65−67. Although only the second and third residue are conserved, the tripeptide is always located within a helical segment that traverses the center of the protein (Figure 1A). The protein fold encourages nucleophilic attack of the Gly67 amide nitrogen on the carbonyl carbon of Ser65 (species a in Scheme 1), creating a heterocyclic structure from the backbone atoms of the three residues (species b in Scheme 1). The cyclization reaction is promoted by the electrostatic catalyst Arg96, and subsequent removal of the Tyr66 α-proton is likely facilitated by the acid−base catalyst Glu222 (*14*, *15*). The ensuing α-enolate form of the five-member ring (species c and d in Scheme 1) is thought to be reactive to two-electron oxidation by molecular oxygen, generating the cyclic imine form of the protein and hydrogen peroxide as a side product (species e and f in Scheme 1) (*16*). Several years ago, the cyclic imine intermediate was trapped by mutagenesis, and its crystal structure was determined in the hydrated state (e), as well as in several partially dehydrated states (*17*, *18*). Subsequently, deuterium kinetic isotope effect data provided evidence that the cyclic imine undergoes deprotonation at the β-carbon of Tyr66 in a net water elimination process, thereby completing all biosynthetic steps necessary for generating the GFP-like chromophore (species g and h in Scheme 1) (*19*). Although it was long thought that the side chain of Tyr66 mediates the transfer of electrons to molecular oxygen, the kinetic results have repudiated this notion (*16*). Instead, the phenolic group appears to play an essential role in the final dehydration step that contributes to overall rate retardation. Therefore, GFP maturation is best described by a cyclization−oxidation−dehydration sequence of events, where the oxidation step is solely guided by main chain chemistry (*17*). The mature GFP-like chromophore typically emits bright green light in its anionic form (B-form, species h in Scheme 1) and is usually non-fluorescent in its neutral form (A-form, species g in Scheme 1). However, upon excitation of the A-form, green fluorescence may be acquired by excited-state proton transfer (ESPT). In this review, the term "GFP-like chromophore" is used to refer to both protonation states (species g and h in Scheme 1).

DsRed-LIKE PROTEINS: AN ACYLIMINE EXTENSION TO THE CYCLIC IMINE YIELDS A RED-FLUORESCING CHROMOPHORE

In 1999, the research community was surprised by the unforeseen discovery of naturally occurring intense red fluorescence in proteins with distant sequence homology to GFP. At that time, the cloning of six remote cousins of GFP was reported, all originating from a series of Indo-Pacific Anthozoa species (*20*). The most fascinating member of this set of proteins was derived

Scheme 1: Mechanism of Chromophore Formation in Green Fluorescent Protein[a] (*1*, *19*)

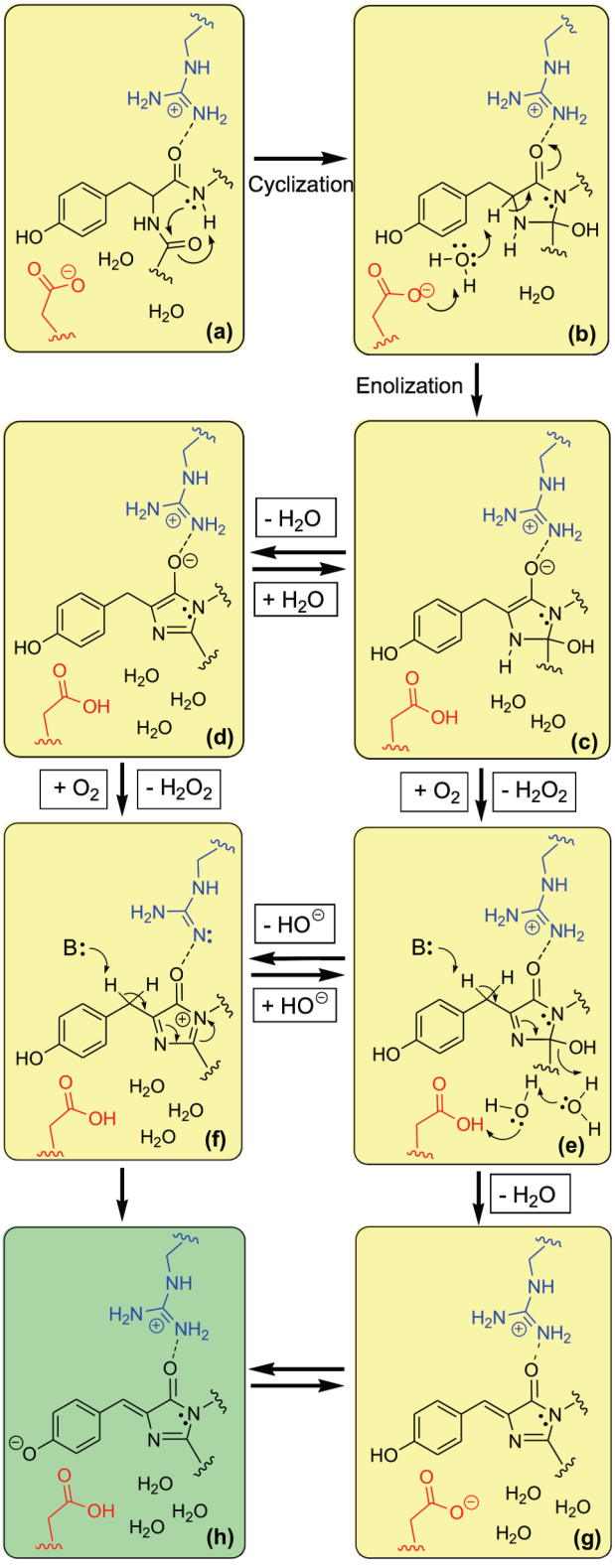

[a]A main chain cyclization reaction (conversion of species (a) to species (b)) initiates the self-modification process and leads to the cyclic α-enolate form that may exist in its hydrated (c) or dehydrated (d) form. Subsequent two-electron oxidation by molecular oxygen yields hydrogen peroxide concomitant with the cyclic imine form of the protein, again either in its hydrated (e) or dehydrated (f) form. In the last step, abstraction of a proton from the tyrosine-derived β-carbon triggers a series of bond rearrangements to yield the mature chromophore, either in its A-form (g), which is neutral, or in its B-form (h), which is anionic. The nature of the base is currently unknown.

from a Discosoma species (Corallimorpharia and Discosomatidae) and exhibited excitation and emission maxima at 558 and 583 nm, respectively. This clone was originally termed drFP583 and was later given the trade name DsRed by Clontech, Inc. Not surprisingly, the unprecedented optical properties attracted immediate and fervent interest in the research community, and several closely related red fluorescent proteins were isolated soon afterward (*21*−*23*). These included nonfluorescent purple chromoproteins, as well as far-red fluorescent proteins with emission maxima at 645 nm (*24*). The purple color was later demonstrated to originate from a conformationally flexible DsRed-like chromophore (*25*).

Biophysical, Biochemical, and Structural Features. Driven by the prospect of developing superior imaging tools, fluorescent protein research underwent a rapid expansion in 2000, as substantial effort was directed toward characterizing the chromophore and protein structure of DsRed. Upon self-assembly into tightly bound homotetramers, color development was observed to progress very slowly over a period of several days (*26*). The mature protein was shown to bear both green and red chromophores in roughly equal amounts (*27*), and time-resolved spectroscopic measurements suggested that intratetramer resonance energy transfer (FRET) may be responsible for the primarily red emission color (*28*, *29*).

Before an X-ray structure of DsRed became available, the chemical form of the fully mature red chromophore was elucidated by mass spectrometric techniques (*27*). On the basis of these data, an acylimine extension to the two-ring π-system of the GFP-like chromophore was proposed, as supported by theoretical calculations (species f in Scheme 2). In line with the known susceptibility of acylimines to acid−base hydrolysis, acid denaturation was shown to produce two peptide fragments (*27*). In combination, the results supported a chemical structure that involved Gln66 dehydrogenation at the C_α−N main chain bond located directly adjacent to the chromophore's heterocycle, thus extending the π-orbital delocalization by an additional loss of two hydrogen atoms along the backbone. The maturation process was demonstrated to critically depend on molecular oxygen, as hydrogen peroxide could not be substituted as an oxidant (*27*).

Immediately following the elucidation of the chemical nature of the DsRed chromophore, two papers reported the high-resolution protein X-ray structure (*30*, *31*). Both noted a trigonal planar geometry of the α-carbon of Gln66, in conjunction with a highly unusual geometry that appeared to suggest a *cis* peptide bond connecting Phe65 with Gln66 (Figure 2A). The electron density provided evidence of sp^2 hybridization of C_α66, in strong support of an acylimine being the distinguishing feature of red fluorescence (*27*). Crystallographic refinement to 1.3 Å suggested that only approximately half of the protein chains in the crystal bear a desaturated C_α66−N65 bond (*30*), confirming the coexistence of green and red chromophores at the end point of red fluorescence acquisition. Notably, the X-ray structures provided a rationale for the reported pH insensitivity of red fluorescence (*26*), based on ion pairing of the chromophore's phenolate oxygen with the ε-amino group of Lys163 (*30*, *31*).

Mechanistic Hypothesis for Main Chain Oxidation: A Carbanion-like Intermediate Followed by a Hydroperoxy Adduct? An early formulation of the DsRed maturation mechanism suggested that the GFP-like population observed in immature DsRed constitutes an intermediate form from which the red species is generated (*27*). Although the sequence of steps in

Scheme 2: Proposed Mechanism for DsRed Chromophore Biogenesis According to Strack et al. (*32*)[a]

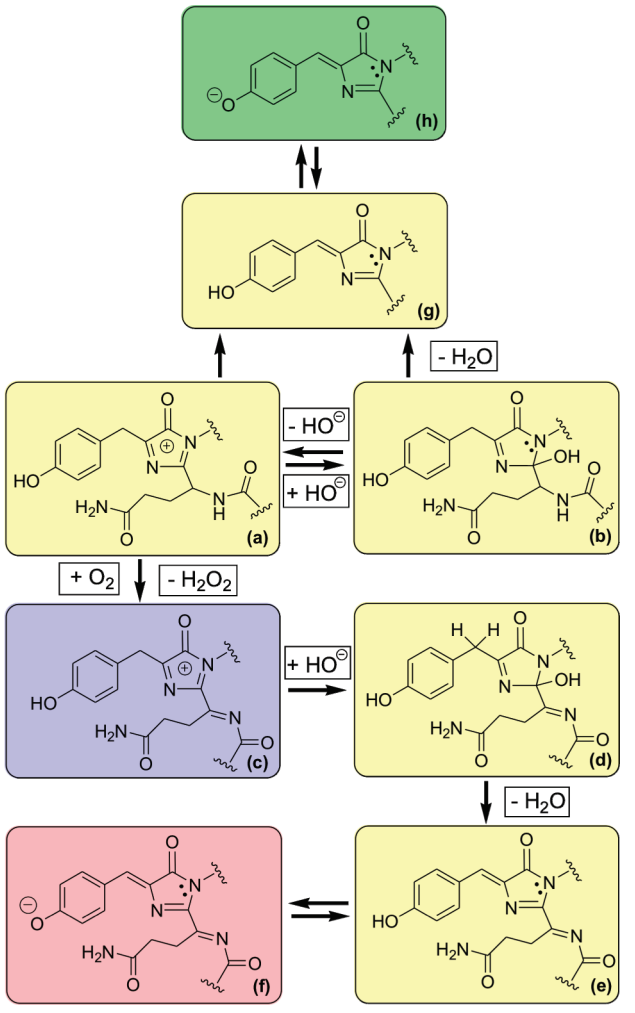

[a]The cyclic imine intermediate is generated according to Scheme 1 (*17*) and may exist in its cationic (a) or hydroxylated (b) form. The intermediate (a) serves as the branch point between green and red pathways. The green pathway leads to the GFP-like chromophore shown as structures (g) and (h), whereas the red pathway leads to the red fluorescent chromophore (f). The red chromophore is produced from species a via air oxidation to generate the acylimine (species (c)), followed by hydroxylation to yield species (d), and subsequent β-carbon deprotonation to generate species (e) and (f). Proposed details of air oxidation are shown in Figure 2.

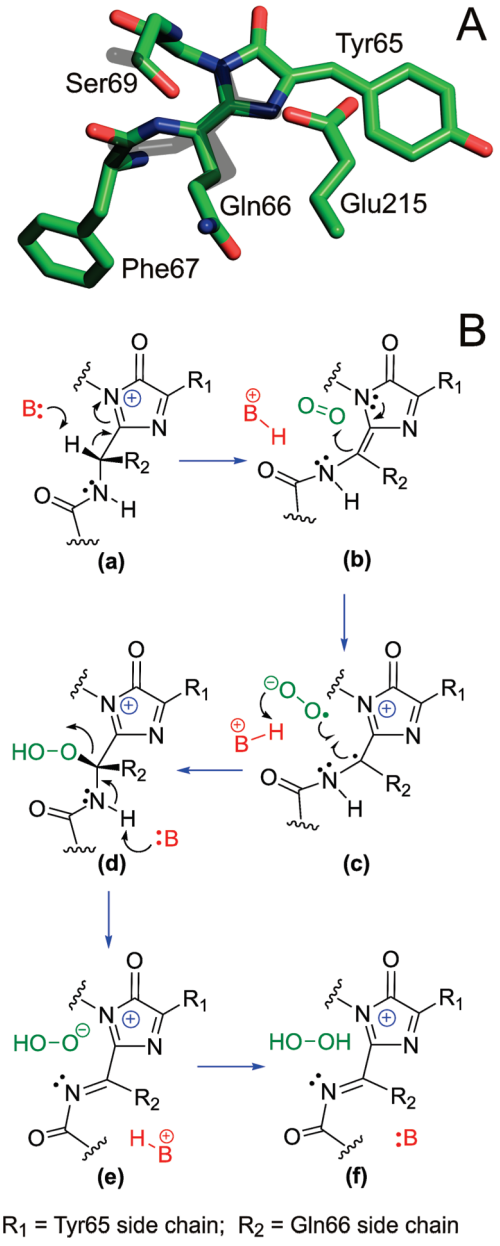

FIGURE 2: (A) X-ray structures of green and red forms of DsRed coexisting in the same crystal (*35*). Gray indicates the GFP-like green fluorescent chromophore. Atom colors for the DsRed red fluorescent chromophore: green for C, red for O, and blue for N. (B) Proposed chemistry of acylimine formation according to Yarbrough et al. (*30*), shown in the same orientation as the crystal structure. The O_2-reactive moiety has been proposed to be the cyclic imine form a (*32*). The mechanism follows that proposed for cyclic imine formation by Rosenow et al. (*17*). Proton abstraction according to species (a) yields either a carbanionic or neutral species (b), which transfers one electron to O_2, producing the superoxide anion radical concomitant with a protein-based radical species (c). Radical−radical combination and protonation produce the hydroperoxy adduct (d), followed by peroxide anion elimination to yield the acylimine-extended form (e), followed by equilibration of protonation states to provide species f, which is identical to species (c) in Scheme 2. The identity of proton donors and acceptors is unknown; B stands for base.

this mechanistic outline has recently been revised (see below) (*32*−*34*), the original hypothesis put forth for the mechanism of main chain oxidation remains viable (Figure 2B) (*30*). Air oxidation was proposed to be triggered by proton abstraction at C_α66, likely mediated by Glu215 as the catalytic base (species a in Figure 2B), such that a carbanion-like intermediate is generated that is stabilized by charge delocalization over the heterocycle (species b in Figure 2B). Although Ser69 was originally invoked as a participant in general base catalysis, this residue was later shown to be noncritical (*35*, *36*).

The subsequent protein oxidation steps were proposed to involve a transient hydroperoxy adduct as shown in species d in Figure 2B (*30*). To generate this adduct, species b is thought to transfer an electron to O_2, producing a superoxide anion radical and a protein-based radical species as shown in species c. Subsequently, radical−radical combination and proton transfer may produce hydroperoxy adduct d. Upon peroxide elimination, the resulting acylimine-extended moiety e may equilibrate to species f, which is identical to species c in Scheme 2. This type of ground-state oxidation mechanism has previously been proposed for cyclic imine formation during GFP maturation (Scheme 1) (*17*). Ample precedence for the direct activation of O_2 by protein-bound

organic groups is provided by the non-metallo oxidase group of enzymes, enzymes that utilize flavins, pterins, or quinones as organic cofactors (*37*). Within this group, glucose oxidase may be considered a prototype in catalyzing the energetically difficult one-electron reduction of O_2 to superoxide. Another example is provided by the luciferases, such as aequorin, in which the coelenterazine substrate was shown to be bound as a hydroperoxy adduct (*38*).

Although in DsRed, the identity of proton donors and acceptors is not currently known, the protein fold provides several positive charges that may help stabilize a carbanion-like intermediate and the ensuing superoxide anion. One possible scenario involves a positively charged cyclic imine as the reactive moiety (Figure 2B) (*32*), rendering species b net neutral (see below).

Cyclic Imine as a Branch Point for the Development of Green and Red Chromophores. The first detailed kinetic analysis of DsRed maturation was reported in 2004, describing a nonfluorescent intermediate with maximal light absorption at 408 nm (*39*). On the basis of its absorbance characteristics and blue appearance, this species was originally proposed to be identical to the neutral form of the GFP-like chromophore (species g in Scheme 1). Global curve fitting of several kinetic progress curves provided support for a branched model, in which the protonated chromophore was proposed to represent a common intermediate from which the green and red forms would be derived (*39*). Although the overall outline of a branched mechanism has recently been confirmed, the exact branch point and the chemical identity of the blue species have been revised (see below) (*32*−*34*).

The notion of a GFP-like chromophore as an obligatory intermediate on the pathway of red fluorescence acquisition was almost universally accepted for nearly a decade (*40*). In spite of the rather appealing nature of this idea, two different groups have provided convincing arguments that repudiate this basic tenet of fluorescent protein maturation (*32*, *33*). On the basis of a comparison of X-ray structures of DsRed-type fluorescent timer variants that included a trapped blue species and a fully mature red version, Pletnev et al. proposed that the biosynthetic pathway proceeds via a blue intermediate bearing an acylimine extension to the five-member heterocycle (*33*). This blue form was described as being devoid of π-conjugation to the phenolic group, suggesting that acylimine formation precedes desaturation of the tyrosine $C_\alpha-C_\beta$ bond (*33*). Additional X-ray structures consistent with this proposal include that of mTagBFP, an engineered blue fluorescent protein derived from DsRed. This structure more clearly indicates the noncoplanar, almost perpendicular nature of the Tyr64 phenolic group in relation to the main chain-derived heterocycle, while the α-carbon of the preceding residue adopts a trigonal planar geometry, consistent with main chain dehydrogenation that yields the acylimine (*34*). Mass spectrometric data on chromophore-bearing proteolytic peptides appeared to support the notion that the five-member ring remains fully reduced and exists in its enolic and dehydrated form. According to Pletnev et al., the blue species would be that of the cyclic enolate shown as species d in Scheme 1, with the addition of an adjacent carbon−nitrogen double bond (*34*). Therefore, the proposed mechanism is similar but not identical to the mechanism depicted in Scheme 2, where the blue intermediate (c) is shown in the cyclic imine form instead of the α-enolate form (see below). Currently, we do not know whether the mTagBFP end state characterized by crystallographic and mass spectrometric techniques represents a trapped version of an on-pathway intermediate for DsRed maturation (*34*).

Almost simultaneously, a somewhat different mechanism for DsRed maturation was proposed by Strack et al., who suggested that the biosynthetic pathway splits into two branches at the two-electron oxidized cyclic imine stage (species a in Scheme 2) (*32*). According to this proposal, the colorless imine form represents the last common intermediate from which two different pathways lead to either the green or the red chromophore. The green form may be generated as proposed previously (Scheme 1) (*19*), whereas maturation of the red branch may involve two additional long-lived intermediates (c and d in Scheme 2). Most notable is the blue intermediate along the red branch that consists of the oxidized cyclic imine in conjugation with an acylimine. This particular aspect suggests that two-electron oxidation of the heterocycle may trigger a subsequent two-electron main chain oxidation, with each of the two steps reducing one molecule of O_2 to H_2O_2 (Scheme 2).

By monitoring the time evolution of hydrogen peroxide production during protein maturation, Strack et al. (*32*) have elegantly expanded on an experimental approach established previously for GFP (*16*). In this way, they have demonstrated that about two H_2O_2 molecules evolve for each red chromophore generated (*32*), providing strong evidence that H_2O_2 evolution occurs prior to the rise of blue fluorescence (Scheme 2). Therefore, the kinetic data presented allow for a more precise ordering of steps, in line with heterocyclic oxidation to yield species a occurring prior to acylimine formation to yield species c. Therefore, the enolate form is less likely to serve as branch point in DsRed maturation.

The model developed by Strack et al. is in part based on kinetic isotope effect studies that utilize biosynthetic incorporation of C_β-dideuterated tyrosine, following a method previously established for GFP (*19*). The authors succeed in demonstrating that both the green and red pathways conclude with a proton abstraction step at the β-carbon of the central tyrosine residue (species d in Scheme 2). Therefore, only the final, postoxidation step seems to effectively incorporate the tyrosine-derived phenolic group into the chromophore's π-system (Tyr67 in DsRed) (*32*). The authors report that this step is partially rate-determining along both green and red pathways. Thus, the mechanistic model presented is able to account for all experimental observations related to the complex maturation process of DsRed (Scheme 2) (*32*).

Peptide Bond Isomerization Might Not Play a Role in Main Chain Oxidation. When the first two DsRed crystal structures were described, the modified peptide bond connecting Phe65 with Gln66 was reported to adopt an unusual conformation (*30*, *31*). Although the term "*cis* peptide bond" was used in both original reports and has since been propagated throughout the literature (*35*), this term may not describe the chemistry appropriately, because the amide linkage has been modified by oxidation (Scheme 2). The acylimine product bears a trigonal planar Gln66 α-carbon (Figure 2A, colored green) generated from the tetrahedral precursor form (Figure 2A, colored gray) by net C−N bond dehydrogenation. The chirality of the L-amino acid precursor dictates that the α-proton should point "up" in the orientation shown. Therefore, proton abstraction as shown in species a, and hydroperoxy adduct formation as shown in species d, must occur from the "upper" face of the nascent chromophore, in the proximity of the carboxyl of Glu215 (Figure 2B). β-Elimination of a hydroperoxide to yield species e would flatten

the C_α66 geometry to a trigonal planar form, such that structural relaxation may provide the observed geometry of the mature form f. The substantial double-bond character of the original peptide bond is expected to be diminished in the acylimine form, as the nitrogen lone electron pair occupies an orbital orthogonal to the imine π-system, reducing orbital overlap with the carbonyl group. For these reasons, invoking a *cis* peptide bond precursor to the acylimine seems poorly justified. In fact, if such isomerization was to occur upon protein folding, the acylimine carbonyl oxygen would likely be pointing "down", not up as observed (Figure 2A,B).

Although an early computational study suggested that the DsRed fold may stabilize a *cis* peptide bond between residues 65 and 66 irrespective of maturation stage (*41*), the notion that all DsRed populations bear a Phe65−Gln66 *cis* peptide bond has since been repudiated (*35*). Indeed, a more recent high-resolution DsRed crystal structure was modeled in two conformations, 50% bearing a normal *trans* peptide bond indicative of the green form and 50% bearing an acylimine component indicative of the red form (Figure 2A). In support of a common mechanism, acylimine-bearing homologues have been shown to exhibit similar geometries (*42*).

Does Photochemistry Partake in the Maturation of DsRed-Type Proteins? In 2004, it was first reported that acquisition of red color could be accelerated by irradiation with a high-power arc lamp (*39*). Although the mechanism remained obscure at the time, subsequent experiments demonstrated that a super-red species forms upon illumination of the acylimine-extended chromophore (*43*). However, this type of photoconversion appeared to be the result of light-induced chromophore *cis*−*trans* isomerization concomitant with decarboxylation of Glu215 (*43*). In line with this notion, more recent work on DsRed-type proteins has provided no evidence in favor of photochemistry as a player in maturation to the red form (*44*). Therefore, the current consensus in the field is that generation of the DsRed chromophore does not depend on light exposure, although subsequent photoinduced optical shifts may be fairly common (*45*). However, these observations do not exclude the possibility that DsRed homologues will be isolated in the future that do depend on light exposure for the acquisition of red fluorescence.

Yellow and Orange FPs Derived from the Acylimine Extension. In some instances, the acylimine bond appears to serve as an electron sink that triggers additional covalent modifications, for example, glutamate or aspartate decarboxylations (*44*, *46*) or acylimine hydrolysis (*47*). Along these lines, a particularly noteworthy example is the nucleophilic addition of the ε-amino group of a lysine residue to the imine carbon atom, generating the yellow fluorescent protein zFP538 in the coral polyp *Zoanthus* (*48*). In this protein, the lysine residue occupying position 66 is thought to generate a cyclic structure by nucleophilic addition onto its own α-carbon, resulting in the ejection of a carboxamide. In this manner, the acylimine appears to be modified to a simple imine, reducing the extent of the chromophore π-system compared to that of DsRed. This feature provides a rationale for the blue-shifted emission maximum of 538 nm for the yellow protein. Other examples of acylimine reactivity have been described, such as the nucleophilic addition of a threonine hydroxyl or a cysteine thiolate onto the acylimine carbonyl carbon, endowing these proteins with orange color, as exemplified by several engineered monomeric orange proteins (*49*, *50*). All known additional self-processing reactions of the DsRed-type chromophore are based on the inherent reactivity of the acylimine group and are frequently coupled to a polypeptide chain break. The mechanistic chemistry of this group of proteins has recently been reviewed (*51*).

GREEN-TO-RED (G/R) PHOTOCONVERTIBLE FPs (KAEDE-LIKE)

Discovery of G/R Photoconversion: Kaede, EosFP, DendFP, and Relatives. Three years after the discovery of DsRed, a unique type of red fluorescence was reported with maturation features entirely distinct from those of DsRed (*52*). In 2002, Miyawaki and co-workers reported the astounding observation that the green-fluorescing form of a newly cloned GFP-like protein was modified to a bright red species when exposed to sunlight. This protein, derived from the stony coral *Trachyphyllia geoffroyi*, was termed Kaede (maple leaf in Japanese), based on the observation that G/R color conversion appeared to be triggered by UV or violet light (*52*). The irreversible red shift in emission from 518 nm (green) to 582 nm (red) occurred with a low quantum yield of 2.4×10^{-4} upon 400 nm light exposure (*52*).

Shortly afterward, Nienhaus and co-workers described a similar photoconversion process in a fluorescent protein termed EosFP from the stony coral *Lobophyllia hemprichii*, a protein with an amino acid sequence 84% identical to that of Kaede (*53*). Subsequently, another close relative termed DendFP from *Dendronephthya* (*6*) was shown to share the same phenomenon of light-induced color modification (*54*). In 2006, an engineered monomeric version, Dendra2, was described to efficiently photoconvert when irradiated with longer-wavelength light such as 488 nm light (*55*). In the same year, the fluorescent proteins mcavRFP and rfloRFP, cloned in 2002 from the great star coral *Monastrea cavernosa* and the corallimorph *Ricordea florida* (*6*), respectively, were shown to acquire red color as a function of light stimulation (*5*). In combination, the experimental evidence strongly suggested that these kinds of proteins are widespread within clade D of the stony corals (Figure 1B).

Light-Induced Main Chain Scission Is Intrinsic to G/R Photoconversion and Requires a Histidine Residue. All known members of the Kaede-type class of red fluorescent proteins bear a His-Tyr-Gly tripeptide at positions 62−64 (Kaede). The histidine residue is critical for the formation of the red chromophore, because its imidazole ring is ultimately incorporated into the three-ring π-system of the mature chromophore (Scheme 3). Support for this notion was provided early by the observation that G/R photoconversion was abolished upon substitution of His62 with phenylalanine, glutamine (*52*), or any other amino acid residue (*56*). In the same study, the chemical structure of the red chromophore was elucidated via application of NMR methods to a five-residue tryptic peptide bearing the chromophore (*56*). The π-conjugated system was shown to include the His62 side chain, based on a desaturated bond between C_α and C_β of His62 (Scheme 3A,B) (*56*). The authors demonstrated further that the A69S substitution in the chromophore environment abolished the photoconversion chemistry, although green color was retained (*56*).

In the absence of an appropriate light source for photochemical modification, the green form of Kaede is the final state of protein self-processing. This form bears a *cis* coplanar two-ring chromophore chemically identical to that found in GFP, likely synthesized in a similar manner and attached to a single polypeptide chain. As originally described for GFP variants (*57*−*59*), the GFP-like chromophore of Kaede is pH-titratable in its

Scheme 3: Hypothetical Mechanism of Red Chromophore Formation in Kaede-Type G/R Photoconvertible Proteins[a]

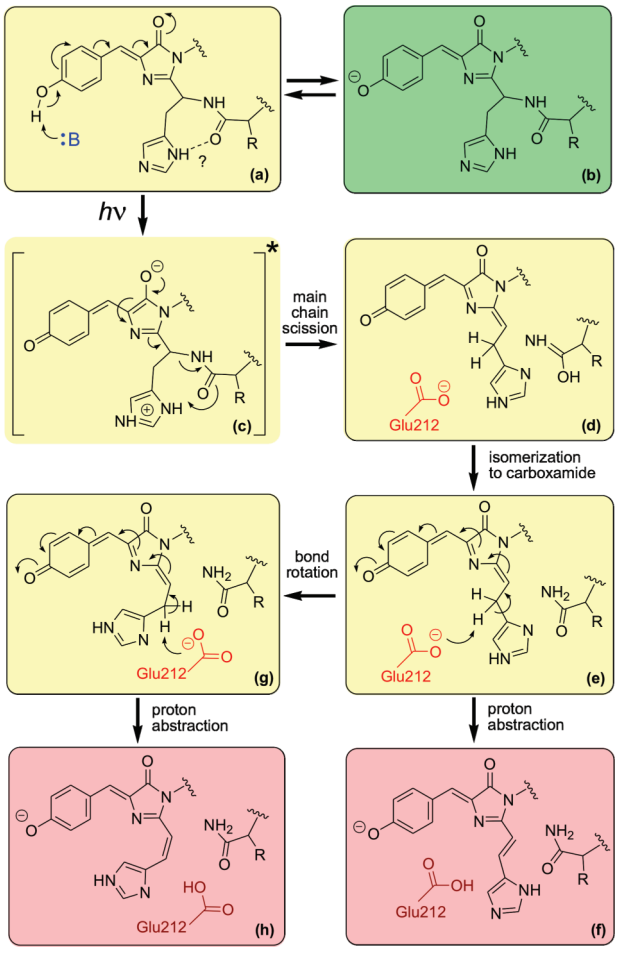

[a]Shown is the two-step (E1-type) mechanism proposed by Mizuno et al. (*56*) and Tsutsui et al. (*66*). The His62 side chain in structure (c) is shown in its cationic form as proposed by Nienhaus et al. (*62*). The overall scheme involves electronic excitation of the neutral GFP-like chromophore a to species (c), which undergoes main chain scission to yield species (d). Isomerization of the ejected leaving group provides for a stable terminal amide group as shown in structure (e). Subsequent deprotonation of the β-carbon of His62 may occur directly from species (e) or may follow bond rotation and occur from species (g). In either case, a red fluorescent three-ring chromophore is generated (species (f) and (h)).

ground state, with the absorbance band at 380 nm arising from the neutral (phenolic) form and the band at 508 nm arising from the anionic (phenolate) form (Scheme 1) (*52*). In 2003, the extraordinary discovery was made that the light-induced chemical changes are coupled to an unusual main chain cleavage reaction occurring in the interior of the β-barrel, without disruption of the tertiary structure (*56*). A careful mass spectrometric analysis of tryptic peptides derived from green and red forms of Kaede led to the identification of His62 as the site for backbone scission, generating two protein chains with respective masses of 10 and 18 kDa. The break in main chain connectivity was inferred to result from an elimination reaction, in which the His62 amide nitrogen is ejected from the adjacent α-carbon (Scheme 3). In addition, the mass spectral results were in line with the formation of a carboxamide group at the newly formed C-terminus of the peptide fragment comprising the N-terminal 10 kDa segment of the precursor chain (Scheme 3) (*56*).

Photoconversion Occurs Only from the Nonfluorescent Form of the GFP-like Chromophore. In their seminal work, Miyawaki and co-workers proposed that electronic excitation of the neutral form of the GFP-like chromophore triggers excited-state deprotonation of its phenolic hydroxyl group (species a in Scheme 3), consistent with ESPT as first described for GFP some years ago (*60*). This process was suggested to produce a transient excited state I* consisting of the chromophore anion, a state that may subsequently decay by β-elimination (conversion of species c to species d in Scheme 3) (*56*). According to this idea, light-activated ejection of the amide leaving group from the His62 α-carbon would yield a hydroxyimino group, a process that would be facilitated by protonation of the Phe61 carbonyl oxygen. This event would be followed by rapid isomerization of the hydroxyimino group to the carboxamide form (species e in Scheme 3) (*56*). Full maturation to the red-emitting form would require an additional step entailing proton abstraction from the β-carbon of His62, such that the ensuing $C_\alpha-C_\beta$ double bond provides for conjugation of the histidine imidazole ring with the remainder of the chromophore skeleton (species f in Scheme 3). The result is a red-emitting three-ring chromophore that experiences reversible protonation−deprotonation equilibria similar to those observed for the green form. The pK_a value of the red species of Kaede was reported to be 5.6 (*52*) and 6.0 (*61*) in separate studies, and as in the green species, steady-state fluorescence emission occurs exclusively from the anionic state of the red chromophore (*61*).

In 2004, clear evidence was provided that only the neutral form of the green state is competent in undergoing light-triggered modification to the red form (*53*). In this work, it was demonstrated that the photochemical action spectrum of EosFP follows the absorption intensity of the GFP-like neutral chromophore almost exactly, consistent with a mechanism in which removal of an excited-state proton from the chromophore's phenolic end may play an essential role (*53*). According to this model, a proton would be transferred from the phenolic side of the chromophore to the imidazole ring of His62 through the protein matrix over a distance of more than 10 Å. This process has been proposed to yield a transient imidazolium cation (species c in Scheme 3) that may serve as proton donor to facilitate the β-elimination reaction (*53*).

Long-range ESPT in G/R photoconversion remains highly controversial. A strong argument against ESPT is the complete lack of green fluorescence upon excitation of the neutral chromophore (*62*). Importantly, a hydrogen-bonded network that would facilitate the transfer of a proton from the chromophore to His62 has not been identified in any of the crystal structures (*62*). To date, ESPT has been demonstrated solely in the red version of Kaede, where the excitation of the protonated three-ring chromophore results in the emission of red light from the anion (*61*). A comparison of crystal structures of the green and red states of EosFP (*62*) and Kaede (*63*) suggests that the H-bonding pattern around the phenolic end remains largely unaffected by photoconversion (Figure 3A), implying that potential proton transfer pathways may be similar in the green and red forms of these proteins. However, no experimental information is available with respect to the nature of the proton acceptor, the long-term residence of the proton upon dissociation from the chromophore, or any solvent equilibration effects.

The pK_a value of green EosFP was shown to be 5.8, very close to that of Kaede, and in line with the higher photoconversion efficiency observed at lower pH values (*53*). Surprisingly, green

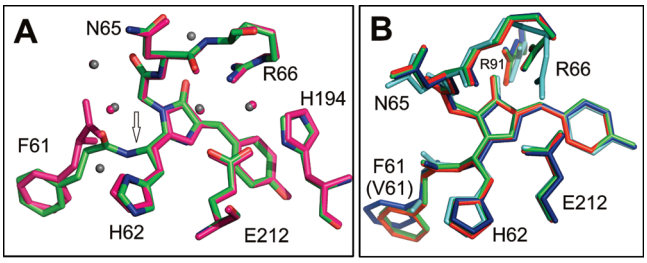

FIGURE 3: (A) Superimposition of EosFP green and red forms (PDB entry 1ZUX colored green and PDB entry 2BTJ colored red). The site of bond scission upon G/R photoconversion is indicated by an arrow. (B) Superimposition of green forms of G/R photoconvertible proteins. The amino acid numbering is that of Kaede (*63*). Green for Kaede (PDB entry 2GW3) (*63*), red for EosFP (PDB entry 1ZUX) (*62*), blue for KikGRX (PDB entry 2DDD) (*66*), and cyan for Dendra2 (PDB entry 2VZX) (*64*).

Dendra2 was shown to exhibit a pK_a value of 7.1, a significantly elevated proton dissociation constant compared to those of EosFP and Kaede, likely a consequence of conformational adjustments of Arg66 (*64*). The pK_a value for the red chromophore of Dendra2 was found to be similarly elevated to 7.5. These values are noteworthy, because they imply that at a solution pH of <7, photoconversion of Dendra2 occurs with a protonated chromophore as both the reactant and product (*64*). This means that a proton released in the excited state would have to rapidly reattach itself to establish the appropriate product equilibrium, eliminating the primary rationale for invoking long-range proton transfer. In further support of a model that lacks ESPT as a mechanistic feature, a recent theoretical study has suggested that the chromophore's phenolic end remains protonated throughout the photochemical reaction progress (*65*).

Structural Preorganization and Glu212 as a General Base for Proton Abstraction. When X-ray structures of green and red forms of EosFP were compared, the unmodified His62 and its oxidized equivalent were found to adopt an almost identical extended side chain conformation (Figure 3A) (*62*). This feature was subsequently confirmed in Kaede (*63*), and structural adjustments due to green-to-red conversion were therefore judged to be minimal in both proteins. In EosFP, a slight rotation of the imidazole group was observed, bringing the ring into the plane of the remainder of the chromophore (Figure 3A), whereas in the green form of Kaede, the imidazole ring was found to be perfectly coplanar with the GFP-like chromophore, suggesting a large degree of structural preorganization. In both proteins, the carboxyl of Glu212 was found to be positioned near the β-carbon of His62 at a distance of 3.3 Å, poised perfectly for general base catalysis in abstraction of a proton from the His62 C_β atom (Scheme 3) (*62*). Convincing support for the function of Glu212 as a general base catalyst was provided by the observation that its replacement with a glutamine abolished red fluorescence entirely (*62*), as was subsequently confirmed with Kaede (*63*).

A few years ago, Nienhaus and co-workers proposed a one-step elimination mechanism, primarily based on the lack of major structural adjustments upon photomodification (*62*). This mechanism is distinct from the previously proposed E1-type mechanism shown in Scheme 3 (*56*), as the deprotonation step at the His62 C_β atom would be responsible for triggering C−N bond cleavage, rather than follow it. An important aspect of such a concerted elimination mechanism is the fact that stereoelectronic control would be provided by the *trans* stereochemistry of the histidine side chain (*62*). However, recent experimental and theoretical work argues against a one-step deprotonation−elimination mechanism (see below) (*65*, *66*). So far, the trapping of intermediate forms of Kaede by mutagenesis has remained unsuccessful, in line with short-lived, unstable intermediate species (Scheme 3) (*63*).

Proposed Role of the His62 Imidazole Group as a Proton Donor. In the crystal structures of the green and red forms of EosFP (*62*), the His62 $N_{\delta 1}$ atom was found to be positioned within hydrogen bonding distance of the Phe61 carbonyl oxygen, whereas in Dendra2, the equivalent distance was increased to 3.6 Å (*64*). On the basis of this observation, Nienhaus and co-workers suggested several years ago that His62 may be the transient acceptor of a light-triggered proton transfer reaction from the phenolic hydroxyl of the chromophore to the imidazole ring (*62*), and that the imidazolium cation would subsequently donate a proton to the main chain carbonyl of Phe61, thus facilitating the elimination reaction (species c in Scheme 3) (*62*). Unfortunately, the hydrogen bonding geometry appears to be somewhat unfavorable, as the carbonyl lone electron pair would be oriented nearly perpendicular to the imidazolium N−H bond proposed to serve as a donor. Miyawaki and co-workers have noted that the green versions of Kaede and EosFP bear a positionally conserved and highly ordered water molecule adjacent to and in plane with the imidazole ring of His62 (Figure 3A) (*63*). Although the hydrogen bonding geometry is not optimal for this interaction either, the additional solvent molecule may aid in stabilizing a transiently charged imidazolium cation.

Recently, computer simulations have been used to shed light on the catalytic role of the imidazole group of His62 (*65*). Using hybrid quantum chemical and molecular mechanical potentials, the theoretical results appear most consistent with a neutral His62 imidazole ring serving as a proton donor to the carbonyl of Phe61, such that a transient imidazolide anion would be generated during the singlet excited state of the chromophore. Subsequently, the system would undergo intersystem crossing to the triplet state, from which peptide bond cleavage would proceed. In the final step, the imidazolide anion would promote abstraction of a proton from C_β, whereas the carboxylate of Glu212 would play the role of an electrostatic catalyst (*65*). Although this mechanism is novel and noteworthy, as it details mechanistic features without invoking phenolic ESPT, the exact catalytic function of His62 as a proton transfer agent remains unresolved, and a passive role for Glu212 in proton abstraction seems unlikely.

Engineering of KikG for G/R Photoconversion Provides Support for a Two-Step Elimination Mechanism. The fact that His62 partakes in the G/R photoconversion machinery (*56*) was exploited in the engineering of a photoactive variant from a natively green protein termed KikG (*67*). First, Asp62 was replaced with a histidine residue, followed by more extensive redesign of the chromophore-bearing pocket to introduce a total of eight substitutions (*67*). The resulting clone, termed KikGR, was demonstrated to undergo highly efficient G/R photoconversion. Unlike Kaede and EosFP, the green chromophore of KikGR was shown to titrate with the surprisingly high pK_a value of 7.8 (*67*). Therefore, the neutral form of the chromophore dominates at physiological pH, providing a rationale for the much improved efficiency of photoconversion. Similar to those of other red forms, the absorbance spectrum of the photomodified chromophore exhibits two maxima at 360 and 583 nm, both

arising from the anion. Excitation of either leads to 593 nm emission with high quantum yields of 0.92 and 0.65, respectively (*67*).

Screening of KikGR mutants for crystallization led to the successful crystallization of a clone termed KikGRX bearing four additional substitutions (*66*). Pre- and postphotoconversion structures were determined, and in its red form, the chromophore of KikGRX was shown to adopt a distinctly *cis* conformation along the desaturated $C_\alpha-C_\beta$ bond of His62 (species h in Scheme 3). This configuration is opposite to the usual *trans* isomers found in all other G/R proteins (species f in Scheme 3). Therefore, the authors have proposed that the rearrangement in the red chromophore structure results from conformational adjustments of an intermediate form generated upon main chain scission. Furthermore, the authors have suggested that in the GFP-like precursor state (species a and b in Scheme 3), rotation around the His62 $C_\alpha-C_\beta$ bond is restricted due to H-bonding of the imidazole ring with the carbonyl oxygen of Phe61 (*66*). The crystal structures of KikGRX are particularly significant, because they include the first structure of a prephotoconversion G/R protein, in which the chromophore is in the neutral state competent in photoconversion (species a in Scheme 3). In this state, the His62 side chain clearly adopts an extended conformation. Therefore, a likely explanation for the *cis* configuration of the red form is a rotation around the saturated $C_\alpha-C_\beta$ bond prior to abstraction of a proton from C_β. The existence of an intermediate with a lifetime that allows for side chain conformational changes provides strong support for a two-step E1-type elimination mechanism (Scheme 3). Once the proton has been removed from Cβ, bond desaturation will provide for full conjugation of the imidazole ring with the remainder of the chromophore π-system; therefore, the conformation will be locked once the protein has fully matured to the red form (species h and f in Scheme 3) (*66*).

GFP "REDDING" PHENOMENA: MYSTERIOUS PHOTOCHEMISTRY

Although light-activated GFP color conversion to a red-emitting form was described more than a decade ago (*68*, *69*), to date, the mechanism of this slow photoactivation process remains unresolved, and the structure of the resulting red chromophore has not been determined yet. In these early studies, red color was reported to develop upon exposure to weak 488 nm laser light under low-oxygen conditions only (*68*). Therefore, this phenomenon was termed "anaerobic redding", in line with the observation that readmittance of air rapidly destroyed the red emission color. Surprisingly, the ability to acquire red fluorescence was shown to occur in a manner independent of the particular GFP variant at hand, and the emission spectrum revealed a high degree of complexity with a series of maxima between 510 and 600 nm, suggesting multiple chromophore populations. Thus, the chemical nature of the anaerobic redding phenomenon remains poorly characterized.

Contrary to anaerobic redding known since 1997 (*68*, *69*), a recent study described a novel photoconversion process that is insensitive to atmospheric conditions (*70*). The photochemistry induced by 488 nm laser light was reported to be fully functional under both aerobic and low-oxygen conditions. This process has been termed "oxidative redding", based on a light-induced electron transfer reaction from the chromophore to various solution components serving as electron acceptors. Compounds tested included ferricyanide (photoconversion quantum yield of ~0.05), benzoquinone, cytochrome *c*, flavin cofactors, and enzymes such as flavin-bearing glucose oxidase. The broad variety of electron acceptors provides support for a model in which electrons are transferred from the electronically excited chromophore through the protein matrix to its surface. The data are consistent with the net transfer of two electrons per chromophore converted from green to red, although the structure of the red chromophore is as yet unknown. Unfortunately, the process was shown to be irreversible, rendering this method unsuitable for dynamic redox reporting in biological applications (*70*).

CONCLUDING REMARKS

In spite of tremendous progress in our understanding of the mechanistic diversity of fluorescence acquisition in GFP-like proteins, many details remain to be elucidated. To develop atomistic models for the variety of self-catalytic post-translational processes that can be accessed by the GFP fold, several important questions need to be addressed. For example, experimental evidence for any of the microscopic steps in the O_2-mediated protein oxidation reactions continues to be lacking. In addition, much controversy exists in the identities and charge states of catalytic groups. The Kaede-type photoconversion mechanism remains poorly established because of the difficulty of trapping intermediates, and alternative mechanisms continue to be proposed. Regardless, the myriad of observed chemistries appear to be based on the intrinsic reactivity of the cyclic imine and acylimine moieties, as well as the rich photochemistry of the GFP-like chromophore. Therefore, it is likely that many more discoveries will be made with respect to spontaneous self-modifications or phototriggered conversions to either generate visible fluorescence or convert one color into another. Intriguingly, further red-shifted versions continue to be discovered, and the long-wave limit seems to be a matter of imagination.

REFERENCES

1. Wachter, R. M. (2007) Chromogenic cross-link formation in green fluorescent protein. *Acc. Chem. Res. 40*, 120–127.
2. Giepmans, B. N. G., Adams, S. R., Ellisman, M. H., and Tsien, R. Y. (2006) Review: The fluorescent toolbox for assessing protein location and function. *Science 312*, 217–224.
3. Shaner, N. C., Patterson, G. H., and Davidson, M. W. (2007) Advances in fluorescent protein technology. *J. Cell Sci. 120*, 4247–4260.
4. Hopf, M., Gohring, W., Ries, A., Timpl, R., and Hohenester, E. (2001) Crystal structure and mutational analysis of a perlecan-binding fragment of nidogen-1. *Nat. Struct. Biol. 8*, 634–640.
5. Matz, M. V., Labas, Y. A., and Ugalde, J. (2006) Evolution of function and color in GFP-like proteins. *Methods Biochem. Anal. 47*, 139–161.
6. Labas, Y. A., Gurskaya, N. G., Yanushevich, Y. G., Fradkov, A. F., Lukyanov, K. A., Lukyanov, S. A., and Matz, M. V. (2002) Diversity and evolution of the green fluorescent protein family. *Proc. Natl. Acad. Sci. U.S.A. 99*, 4256–4261.
7. Alieva, N. O., Konzen, K. A., Field, S. F., Meleshkevitch, E. A., Hunt, M. E., Beltran-Ramirez, V., Miller, D. J., Wiedenmann, J., Salih, A., and Matz, M. V. (2008) Diversity and evolution of coral fluorescent proteins. *PLoS One 3*, e2680.
8. Ugalde, J. A., Chang, B. S. W., and Matz, M. V. (2004) Evolution of coral pigments recreated. *Science 305*, 1433.
9. Field, S. F., Bulina, M. Y., Kelmanson, I. V., Bielawski, J. P., and Matz, M. V. (2006) Adaptive evolution of multicolored fluorescent proteins in reef-building corals. *J. Mol. Evol. 62*, 332–339.
10. Lin, M. Z., McKeown, M. R., Ng, H. L., Aguilera, T. A., Shaner, N. C., Campbell, R. E., Adams, S. R., Gross, L. A., Ma, W., Alber, T., and Tsien, R. Y. (2009) Autofluorescent Proteins with Excitation in the Optical Window for Intravital Imaging in Mammals. *Chem. Biol. 16*, 1169–1179.
11. Ebbinghaus, S., Dhar, A., McDonald, D., and Gruebele, M. (2010) Protein folding stability and dynamics imaged in a living cell. *Nat. Methods 7*, 319–323.

12. Piatkevich, K. D., and Verkhusha, V. V. (2010) Advances in engineering of fluorescent proteins and photoactivatable proteins with red emission. *Curr. Opin. Chem. Biol. 14*, 23–29.
13. Pakhomov, A. A., and Martynov, V. I. (2008) GFP Family: Structural insights into spectral tuning. *Chem. Biol. 15*, 755–764.
14. Sniegowski, J. A., Lappe, J. W., Patel, H. N., Huffman, H. A., and Wachter, R. M. (2005) Base catalysis of chromophore formation in Arg96 and Glu222 variants of green fluorescent protein. *J. Biol. Chem. 280*, 26248–26255.
15. Sniegowski, J. A., Phail, M. E., and Wachter, R. M. (2005) Maturation efficiency, trypsin sensitivity, and optical properties of Arg96, Glu222, and Gly67 variants of green fluorescent protein. *Biochem. Biophys. Res. Commun. 332*, 657–663.
16. Zhang, L., Patel, H. N., Lappe, J. W., and Wachter, R. M. (2006) Reaction progress of chromophore biogenesis in green fluorescent protein. *J. Am. Chem. Soc. 128*, 4766–4772.
17. Rosenow, M. A., Huffman, H. A., Phail, M. E., and Wachter, R. M. (2004) The crystal structure of the Y66L variant of green fluorescent protein supports a cyclization-oxidation-dehydration mechanism for chromophore maturation. *Biochemistry 43*, 4464–4472.
18. Rosenow, M. A., Patel, H. N., and Wachter, R. M. (2005) Oxidative chemistry in the GFP active site leads to covalent cross-linking of a modified leucine side chain with a histidine imidazole: Implications for the mechanism of chromophore formation. *Biochemistry 44*, 8303–8311.
19. Pouwels, L. J., Zhang, L., Chan, N., Dorrestein, P., and Wachter, R. M. (2008) Kinetic isotope effect studies on the de novo rate of chromophore formation in fast- and slow-maturing GFP variants. *Biochemistry 47*, 10111–10122.
20. Matz, M. V., Fradkov, A. F., Labas, Y. A., Savitsky, A. P., Zaraisky, A. G., Markelov, M. L., and Lukyanov, S. A. (1999) Fluorescent proteins from nonbioluminescent Anthozoa species. *Nat. Biotechnol. 17*, 969–973.
21. Fradkov, A. F., Chen, Y., Li, D., Barsova, E. V., Matz, M. V., and Lukyanov, S. A. (2000) Novel fluorescent protein from Discosoma coral and its mutants possesses a unique far-red fluorescence. *FEBS Lett. 479*, 127–130.
22. Wiedenmann, J., Schenck, A., Roecker, C., Girod, A., Spindler, K.-D., and Nienhaus, G. U. (2002) A far-red fluorescent protein with fast maturation and reduced oligomerization tendency from *Entacmaea quadricolor* (Anthozoa, Actinaria). *Proc. Natl. Acad. Sci. U.S.A. 99*, 11646–11651.
23. Petersen, J., Wilmann, P. G., Beddoe, T., Oakley, A. J., Devenish, R. J., Prescott, M., and Rossjohn, J. (2003) The 2.0 Å crystal structure of eqFP611, a far-red fluorescent protein from the sea anemone *Entacmaea quadricolor*. *J. Biol. Chem. 278*, 44626–44631.
24. Gurskaya, N. G., Fradkov, A. F., Terskikh, A. V., Matz, M. V., Labas, Y. A., Martynov, V. I., Yanushevich, Y. G., Lukyanov, K. A., and Lukyanov, S. A. (2001) GFP-like chromoproteins as a source of far-red fluorescent proteins. *FEBS Lett. 507*, 16–20.
25. Willmann, P. G., Petersen, J., Pettikiriarachchi, A., Buckle, A. M., Smith, S. C., Olsen, S., Perugini, M. A., Devenish, R. J., Prescott, M., and Rossjohn, J. (2005) The 2.1 Å crystal structure of the far-red fluorescent protein HcRed: Inherent conformational flexibility of the chromophore. *J. Mol. Biol. 349*, 223–237.
26. Baird, G. S., Zacharias, D. A., and Tsien, R. Y. (2000) Biochemistry, mutagenesis, and oligomerization of DsRed, a red fluorescent protein from coral. *Proc. Natl. Acad. Sci. U.S.A. 97*, 11984–11989.
27. Gross, L. A., Baird, G. S., Hoffman, R. C., Baldridge, K. K., and Tsien, R. Y. (2000) The structure of the chromophore within DsRed, a red fluorescent protein from coral. *Proc. Natl. Acad. Sci. U.S.A. 97*, 11990–11995.
28. Heikal, A. A., Hess, S. T., Baird, G. S., Tsien, R. Y., and Webb, W. W. (2000) Molecular spectroscopy and dynamics of intrinsically fluorescent proteins: Coral red (dsRed) and yellow (Citrine). *Proc. Natl. Acad. Sci. U.S.A. 97*, 11996–12001.
29. Lounis, B., Deich, J., Rosell, F. I., Boxer, S. G., and Moerner, W. E. (2001) Photophysics of DsRed, a red fluorescent protein, from the ensemble to the single molecule level. *J. Phys. Chem. B 105*, 5048–5054.
30. Yarbrough, D., Wachter, R. M., Kallio, K., Matz, M. V., and Remington, S. J. (2001) Refined crystal structure of DsRed, a red fluorescent protein from coral, at 2.0-Å resolution. *Proc. Natl. Acad. Sci. U.S.A. 98*, 462–467.
31. Wall, M. A., Socolich, M., and Ranganathan, R. (2000) The structural basis for red fluorescence in the tetrameric GFP homolog DsRed. *Nat. Struct. Biol. 7*, 1133–1138.
32. Strack, R. L., Strongin, D. E., Mets, L., Glick, B. S., and Keenan, R. J. (2010) Chromophore Formation in DsRed Occurs by a Branched Pathway. *J. Am. Chem. Soc. 132*, 8496–8505.
33. Pletnev, S., Subach, F. V., Dauter, Z., Wlodawer, A., and Verkhusha, V. V. (2010) Understanding blue-to-red conversion in monomeric fluorescent timers and hydrolytic degradation of their chromophores. *J. Am. Chem. Soc. 132*, 2243–2253.
34. Subach, O. M., Malashkevich, V. N., Zencheck, W. D., Morozova, K. S., Piatkevich, K. D., Almo, S. C., and Verkhusha, V. V. (2010) Structural characterization of acylimine-containing blue and red chromophores in mTagBFP and TagRFP fluorescent proteins. *Chem. Biol. 17*, 333–341.
35. Tubbs, J. L., Tainer, J. A., and Getzoff, E. D. (2005) Crystallographic structures of Discosoma red fluorescent protein with immature and mature chromophores: Linking peptide bond trans-cis isomerization and acylimine formation in chromophore maturation. *Biochemistry 44*, 9833–9840.
36. Strongin, D. E., Bevis, B., Khuong, N., Downing, M. E., Strack, R. L., Sundaram, K., Glick, B. S., and Keenan, R. J. (2007) Structural rearrangements near the chromophore influence the maturation speed and brightness of DsRed variants. *Protein Eng., Des. Sel. 20*, 525–534.
37. Klinman, J. P. (2007) How do enzymes activate oxygen without inactivating themselves? *Acc. Chem. Res. 40*, 325–333.
38. Head, J. F., Inouye, S., Teranishi, K., and Shimomura, O. (2000) The crystal structure of the photoprotein aequorin at 2.3 Å resolution. *Nature 405*, 372–376.
39. Verkhusha, V., Chudakov, D. M., Gurskaya, N. G., Lukyanov, S., and Lukyanov, K. A. (2004) Common pathway for the red chromophore formation in fluorescent proteins and chromoproteins. *Chem. Biol. 11*, 845–854.
40. Wachter, R. M. (2006) The family of GFP-like proteins: Structure, function, photophysics and biosensor applications. *Photochem. Photobiol. 82*, 339–344.
41. Zaveer, M. S., and Zimmer, M. (2003) Structural analysis of the immature form of the GFP homologue DsRed. *Bioorg. Med. Chem. Lett. 13*, 3919–3922.
42. Pakhomov, A. A., Pletneva, N., Balashova, T. A., and Martynov, V. I. (2006) Structure and reactivity of the chromophore of a GFP-like chromoprotein from *Condylactis gigantea*. *Biochemistry 45*, 7256–7264.
43. Habuchi, S., Cotlet, M., Gensch, T., Bednarz, T., Haber-Pohlmeier, S., Rozenski, J., Dirix, G., Michiels, J., Vanderleyden, J., Heberle, J., De Schryver, F. C., and Hofkens, J. (2005) Evidence for the isomerization and decarboxylation in the photoconversion of the red fluorescent protein DsRed. *J. Am. Chem. Soc. 127*, 8977–8984.
44. Pakhomov, A. A., and Martynov, V. I. (2007) Chromophore aspartate oxidation-decarboxylation in the green-to-red conversion of a fluorescent protein from *Zoanthus* sp. 2. *Biochemistry 46*, 11528–11535.
45. Kremers, G. J., Hazelwood, K. L., Murphy, C. S., Davidson, M. W., and Piston, D. W. (2009) Photoconversion in orange and red fluorescent proteins. *Nat. Methods 6*, 355–358.
46. Pletneva, N., Pletnev, S., Tikhonova, T., Popov, V., Martynov, V., and Pletnev, V. (2006) Structure of a red fluorescent protein from *Zoanthus*, zRFP574, reveals a novel chromophore. *Acta Crystallogr. D62*, 527–532.
47. Quillin, M. L., Anstrom, D. M., Shu, X., O'Leary, S., Kallio, K., Chudakov, D. M., and Remington, S. J. (2005) Kindling fluorescent protein from *Anemonia sulcata*: Dark-state structure at 1.38 Å resolution. *Biochemistry 44*, 5774–5787.
48. Remington, S. J., Wachter, R. M., Yarbrough, D. K., Branchaud, B. P., Anderson, D. C., Kallio, K., and Lukyanov, K. A. (2005) zFP538, a yellow fluorescent protein from *Zoanthus*, contains a novel three-ring chromophore. *Biochemistry 44*, 202–212.
49. Shu, X., Shaner, N. C., Yarbrough, C. A., Tsien, R. Y., and Remington, S. J. (2006) Novel chromophores and buried charges control color in mFruits. *Biochemistry 45*, 9639–9647.
50. Kikuchi, A., Fukumura, E., Karasawa, S., Mizuno, H., Miyawaki, A., and Shiro, Y. (2008) Structural Characterization of a Thiazoline-Containing Chromophore in an Orange Fluorescent Protein, Monomeric Kusabira Orange. *Biochemistry 47*, 11573–11580.
51. Pakhomov, A. A., and Martynov, V. I. (2009) Posttranslational chemistry of proteins of the GFP family. *Biochemistry* (*Moscow, Russ. Fed.*) *74*, 250–259.
52. Ando, R., Hama, H., Yamamoto-Hino, M., Mizuno, H., and Miyawaki, A. (2002) An optical marker based on the UV-induced green-to-red photoconversion of a fluorescent protein. *Proc. Natl. Acad. Sci. U.S.A. 99*, 12651–12656.
53. Wiedenmann, J., Ivanchenko, S., Oswald, F., Schmitt, F., Roecker, C., Salih, A., Spindler, K.-D., and Nienhaus, G. U. (2004) EosFP, a fluorescent marker protein with UV-inducible green-to-red fluorescence conversion. *Proc. Natl. Acad. Sci. U.S.A. 101*, 15905–15910.

54. Pakhomov, A. A., Martynova, N. Y., Gurskaya, N. G., Balashova, T. A., and Martynov, V. I. (2004) Photoconversion of the chromophore of a fluorescent protein from Dendronephthya sp. *Biochemistry* (*Moscow, Russ. Fed.*) *69*, 901–908.
55. Gurskaya, N. G., Verkhusha, V. V., Shcheglov, A. S., Staroverov, D. B., Chepurnykh, T. V., Fradkov, A. F., Lukyanov, S., and Lukyanov, K. A. (2006) Engineering of a monomeric green-to-red photoactivatable fluorescent protein induced by blue light. *Nat. Biotechnol. 24*, 461–465.
56. Mizuno, H., Mal, T. K., Tong, K. I., Ando, R., Furuta, T., Ikura, M., and Miyawaki, A. (2003) Photo-induced peptide cleavage in the green-to-red conversion of a fluorescent protein. *Mol. Cell 12*, 1051–1058.
57. Tsien, R. Y. (1998) The Green Fluorescent Protein. *Annu. Rev. Biochem. 67*, 509–544.
58. Elsliger, M.-A., Wachter, R. M., Hanson, G. T., Kallio, K., and Remington, S. J. (1999) Structural and spectral response of green fluorescent protein variants to changes in pH. *Biochemistry 38*, 5296–5301.
59. Wachter, R. M., Yarbrough, D., Kallio, K., and Remington, S. J. (2000) Crystallographic and energetic analysis of binding of selected anions to the yellow variants of green fluorescent protein. *J. Mol. Biol. 301*, 159–173.
60. Chattoraj, M., King, B. A., Bublitz, G. U., and Boxer, S. G. (1996) Ultra-fast excited state dynamics in Green Fluorescent Protein: Multiple states and proton transfer. *Proc. Natl. Acad. Sci. U.S.A. 93*, 8362–8367.
61. Hosoi, H., Mizuno, H., Miyawaki, A., and Tahara, T. (2006) Competition between energy and proton transfer in ultrafast excited-state dynamics of an oligomeric fluorescent protein Kaede. *J. Phys. Chem. B 110*, 22853–22860.
62. Nienhaus, K., Nienhaus, G. U., Wiedenmann, J., and Nar, H. (2005) Structural basis for photo-induced protein cleavage and green-to-red conversion of fluorescent protein EosFP. *Proc. Natl. Acad. Sci. U.S.A. 102*, 9156–9159.
63. Hayashi, I., Mizuno, H., Tong, K. I., Furuta, T., Tanaka, F., Yoshimura, M., Miyawaki, A., and Ikura, M. (2007) Crystallographic evidence for water-assisted photo-induced peptide cleavage in the stony coral fluorescent protein Kaede. *J. Mol. Biol. 2007*, 918–926.
64. Adam, V., Nienhaus, K., Bourgeois, D., and Nienhaus, G. U. (2009) Structural basis of enhanced photoconversion yield in green fluorescent protein-like protein Dendra2. *Biochemistry* (*Moscow, Russ. Fed.*) *48*, 4905–4915.
65. Lelimousin, M., Adam, V., Nienhaus, G. U., Bourgeois, D., and Field, M. J. (2009) Photoconversion of the fluorescent protein EosFP: A hybrid potential simulation study reveals intersystem crossings. *J. Am. Chem. Soc. 131*, 16814–16823.
66. Tsutsui, H., Shimizu, H., Mizuno, H., Nukina, N., Furuta, T., and Miyawaki, A. (2009) The E1 Mechanism in Photo-Induced β-Elimination Reactions for Green-to-Red Conversion of Fluorescent Proteins. *Chem. Biol. 16*, 1140–1147.
67. Tsutsui, H., Karasawa, S., Shimizu, H., Nukina, N., and Miyawaki, A. (2005) Semi-rational engineering of a coral fluorescent protein into an efficient highlighter. *EMBO Rep. 6*, 233–238.
68. Elowitz, M. B., Surette, M. G., Wolf, P.-E., Stock, J., and Leibler, S. (1997) Photoactivation turns green fluorescent protein red. *Curr. Biol. 7*, 809–812.
69. Sawin, K. E., and Nurse, P. (1997) Photoactivation of green fluorescent protein. *Curr. Biol. 7*, R606–R607.
70. Bogdanov, A. M., Mishin, A. S., Yampolsky, I. V., Belousov, V. V., Chudakov, D. M., Subach, F. V., Verkhusha, V. V., Lukyanov, S., and Lukyanov, K. A. (2009) Green fluorescent proteins are light-induced electron donors. *Nat. Chem. Biol. 5*, 459–461.